Eur. Phys. J. A **1**, 299–306 (1998)

THE EUROPEAN PHYSICAL JOURNAL A

The comparison of characteristics of π^- mesons produced in central Mg-Mg interactions with the quark gluon string model predictions

L. Chkhaidze, T. Djobava, L. Kharkhelauri, M. Mosidze

High Energy Physics Institute, Tbilisi State University, University St 9, 380086 Tbilisi, Republic of Georgia, (Fax: (99532) 99-06-89; e-mail: djobava@sun20.hepi.edu.ge or, ida@sun20.hepi.edu.ge

Received: 2 August 1997 / Revised version: 17 November 1997
Communicated by V. Metag

Abstract. A detailed study of pion production in central Mg-Mg collisions at a momentum of 4.3 GeV/c per incident nucleon was carried out with use of the setup GIBS. The average kinematical characteristics of pions (multiplicity n_-, momentum P, transverse momentum P_T, emission angle Θ, rapidity Y) and corresponding distributions have been obtained. The experimental results have been compared with the predictions of the Quark Gluon String Model (QGSM) and satisfactory agreement between the experimental data and the model has been found. The QGSM reproduces also the dependence of average P_T on n_-. The temperatures of π^- mesons have been estimated in the rapidity interval of $0.5 \leq Y \leq 2.1$. A satisfactory fit for π^- mesons has been achieved by using a form involving two temperatures T_1 and T_2. It is found that the QGSM underestimates T_2 by $(10-15)\%$.
The data have been analyzed using the transverse momentum technique. The observed dependence of the $< P_x'(Y) >$ on Y shows the S-shape behaviour. The slope at midrapidity F has been determined. The QGSM reproduces the $< P_x >$ distribution satisfactorily, but underestimates the parameter F.

PACS. 25.70.-z Low and intermediate energy heavy-ions reactions – 25.75.Ld Collective flow

1 Introduction

Relativistic nucleus-nucleus collisions are very well suited for the investigation of excited nuclear matter properties which are the subject of intense studies both experimentally and theoretically. The theoretical models predict the formation of exotic states of nuclear matter.

The experimental discovery of such states is impossible without understanding the mechanism of collisions and studying the characteristics of multiparticle production in nucleus-nucleus interactions.

The purpose of the present article is to study properties of π^- mesons , produced in Mg-Mg collisions with the set-up GIBS, which is the modified version of the set-up SKM-200 [1]. The choice of π^- mesons is due to the fact, that they are dominantly produced particles; they carry information about the dynamics of collisions and can be unambiguously identified among other reaction products. It should be noted also, that the production of π^- mesons is the predominant process at energies of the Dubna synchrophasotron.

In previous articles [1,2] we studied the characteristics of π^- mesons in collisions of various pairs of nuclei (He-Li, He-C, C-C, C-Ne, O-Ne, Ne-Ne, C-Cu, C-Pb and O-Pb) and also the results based on the part of experimental data of Mg-Mg interactions (1390 interactions, 10414- π^- mesons) had been obtained. In paper [3] a good agreement of the CASIMIR (CAScade Intranuclear Made In Rossendorf) cascade model calculations with Mg-Mg interactions (6239 collisions – 50750 π^- mesons) experimental data on inclusive characteristics and correlations of secondaries was shown. In this paper we have used the next generation of intranuclear cascade models – the Quark Gluon String Model (QGSM) [4,5] for comparison with experimental data. It is assumed that interactions of identical nuclei (Mg-Mg) give the possibility of better manifestation of nuclear effects than the interactions of asymmetric pairs of nuclei.

2 Experiment

The data were obtained using a 4π spectrometer SKM-200 — GIBS of the Dubna Joint Institute for Nuclear Research. The facility consists of a 2 m streamer chamber with the fiducial volume $2\times1\times0.6$ m^3, placed in a magnetic field of ~ 0.9 T and a triggering system. The streamer chamber was exposed to beam of Mg nuclei accelerated in the synchrophasotron up to a momentum of 4.3 GeV/c per incident nucleon. The solid target (Mg) in the form of a thin disc (with thickness 1.5 g/cm^2) was mounted inside the chamber at a distance of 70 cm

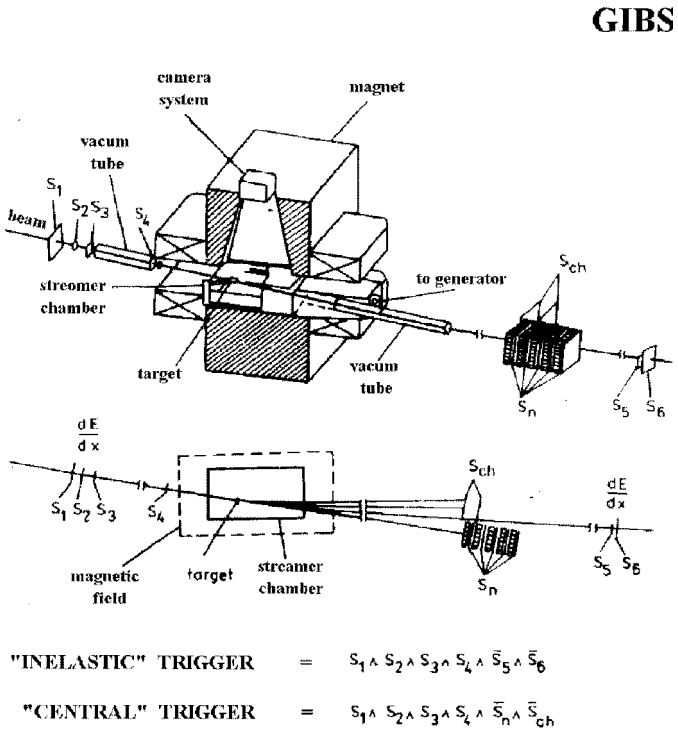

Fig. 1. Experimental set-up. The trigger and the trigger distances are not to scale

from the entrance window and at a height of 8 cm above the middle electrode. The photographs of the events were taken using an optical system with 3 objectives. The experimental set-up and the logic of the triggering system are presented in Fig. 1. The triggering system allowed the selection of "inelastic" and "central" collisions.

The "inelastic" trigger, consisting of two sets of scintillation counters mounted upstream (S_1 - S_4) and downstream (S_5, S_6) the chamber, has been selecting all inelastic interactions of incident nuclei on a target.

The "central" triggering system was consisting of the same upstream part as in the "inelastic" system and of scintillation veto counters (S_{ch}, S_n), registering a projectile and its charged and neutral spectator fragments, in the downstream part. All counters were made from plastic scintillators and worked with photomultipliers PM-30. The S_1 counter with the scintillator of 20×20×0.5 cm^3 size, worked in the amplitude regime and identified the beam nuclei by its charge. The nuclei from the beam, going to the target, have been selected using the profile counters S_2, S_3 with the plastic of 15 mm diameter and 3 mm thickness and "thin" counter S_4 (15 mm and 0.1 mm correspondingly). The S_{ch} counters (two counters with plastic of 40×40×0.5 cm^3 size) were placed at a distance of 4 m downstream from the target and registered the secondary charged particles, emitted from the target within a cone of half angle Θ_{ch}=2.4^0. The S_n counters were registering the neutrons, emitted from the target in the same solid angle Θ_n=2.4^0. The S_n telescope consisted of the five counters of 40×40×2 cm^3 size, layered by 10 cm thick iron blocks. Thus, the trigger was selecting central collision events defined as those without charged projectile spectator fragments and spectator neutrons (P/Z > 3 GeV/c) emitted at angles Θ_{ch}=Θ_n=2.4^0 ($\sim$ 4 msr) which corresponds to a stripping nucleon transverse momentum of $\sim$ 180 MeV/c. The trigger efficiency was 99 % and 80 % for charged and neutral projectile fragments, respectively. The trigger mode for each exposure is defined as T(Θ_{ch} ,Θ_n) (where Θ_{ch} ,Θ_n are expressed in degrees and rounded to the closest integer value). Thus Mg-Mg interactions obtained with this set-up correspond to the trigger T(2,2). The fraction of such events is $\approx 4{\cdot}10^{-4}$ among all inelastic interactions.

Approximately 10% of π^- mesons are lost mainly due to absorption in the target and bad measurability of vertical tracks which are localized around a target rapidity value of -1.1 in the Mg-Mg rest frame. This leads to a shift of the mean π^- rapidity by +0.1 relative to Mg-Mg c.m.s. Average measurement errors of the momentum and production angle determination for $\pi-$ mesons are $\Delta P/P$ = 1.5%, $\Delta\theta$ = 0.3^0.

3 Quark gluon string model

In the study of nucleus-nucleus collisions at high energy several theoretical models have been proposed [6]. The models allow one to test various assumptions concerning the mechanism of particle production at extreme conditions achieved only in nucleus-nucleus collisions. The models [7,8] have taken into consideration the decay of baryonic resonances. They showed their usefulness for the interpretation of the experimental data on pion production. The comparison with the calculations of the Quark-Gluon String Model (QGSM) can help us to understand properties of π^- mesons, produced in Mg-Mg collisions as well as to test the validity of the model in general. Below we briefly discuss the main points of the meson production mechanism in the framework of the QGSM.

The model is presented in detail in papers [4,5]. The QGSM is based on the Regge and string phenomenology of particle production in inelastic binary hadron collisions. To describe the evolution of the hadron and quark-gluon phases, the model uses a coupled system of Boltzmann-like kinetic equations. The nuclear collisions are treated as a mixture of independent interactions of the projectile and target nucleons, stable hadrons and short lived resonances. The QGSM includes low mass vector mesons and baryons with spin 3/2, mostly Δ(3/2,3/2) via resonant reactions. Pion absorption by NN quasi – deuteron pairs is also taken into account. The coordinates of nucleons are generated according to a realistic nuclear density. The sphere of the nucleus is filled with the nucleons at a condition that the distance between them is greater than 0.8 fm. The nucleon momenta are distributed in the range of $0 \le P \le P_F$. The maximum nucleon Fermi momentum is

$$P_F = (3\pi^-)^2 h(\rho)^{1/3} \qquad (1)$$

where h = 0.197 fm·GeV/c, ρ(r) is nuclear density.

Table 1. The average kinematical characteristics of π^- mesons

	$\langle n_- \rangle$	$\langle P \rangle$ (GeV/c)	$\langle \Theta \rangle$	$\langle P_T \rangle (GeV/c)$	$\langle Y \rangle$
experiment	8.2±0.1	0.628±0.003	$33.8^0 \pm 0.1^0$	0.229±0.003	1.22±0.03
QGSM b=1.34 fm	8.3±0.1	0.632±0.003	$35.5^0 \pm 0.1^0$	0.237±0.003	1.20±0.02
QGSM $\tilde{b}$	8.1±0.2	0.629±0.005	$36.5^0 \pm 0.3^0$	0.238±0.004	1.18±0.03

The procedure of event generation consists of 3 steps: the definition of configurations of colliding nucleons, production of quark-gluon strings and fragmentation of strings (breakup) into observed hadrons. The model includes also the formation time of hadrons. The QGSM has been extrapolated to the range of intermediate energy ($\sqrt{s} \leq 4$ GeV) to use it as a basic process during the generation of hadron-hadron collisions. The masses of the 'strings' produced at $\sqrt{s} = 3.6$ GeV were small (usually not greater then 2 GeV), and they were fragmenting mainly (≈90%) through two-particle decays. For main NN and πN interactions the following topological quark diagrams [7] were used: binary, 'undeveloped' cylindrical, diffractive and planar. The binary process makes a main contribution which is proportional to $1/P_{lab}$. It corresponds to quark rearrangement without direct particle emission in the string decay. This reaction predominantly results in the production of resonances (for instance, $P + P \rightarrow N + \Delta^{++}$), which are the main source of pions. The comparable contributions to the inelastic cross section, which however decreases with decreasing P_{lab}, come from the diagrams corresponding to the "undeveloped" cylindrical diagrams and from the diffractive processes. The transverse momenta of pions produced in quark-gluon string fragmentation processes are the product of two factors: string motion on the whole as a result of transverse motion of constituent quarks and $q\bar{q}$ production in string breakup. The transverse motion of quarks inside hadrons was described by the Gaussian distribution with variance $\sigma^2 \approx 0.3(\mathrm{GeV/c})^2$. The transverse momenta k_T of produced $q\bar{q}$ pairs in the c.m.s. of the string follow the dependence:

$$W(k_T) = 3B/\pi(1 + Bk_T^2)^4 \qquad (2)$$

where $B = 0.34$ $(\mathrm{GeV/c})^{-2}$.

The cross sections of hadron interactions were taken from experiments. Isotopic invariance and predictions of the additive quark model [9] (for meson-meson cross sections, etc.) were used to avoid data deficiency. The resonance cross sections were assumed to be identical to the stable particle cross sections with the same quark content. For the resonances the tabulated widths were used.

The QGSM simplifies the nuclear effects. In particular, coupling of nucleons inside the nucleus is neglected, and the decay of excited recoil nuclear fragments and coalescence of nucleons is not included.

We have generated Mg-Mg interactions using the Monte-Carlo generator COLLI, which is based on the QGSM. The events have been traced through the detector and trigger filter.

In the generator COLLI there are two possibilities to generate events: 1) at not fixed impact parameter $\tilde{b}$ and 2) at fixed b. The events had been generated for $\tilde{b}$. The number of simulated events is ∼ 4000. From the impact parameter distribution we obtained the mean value of $< b >= 1.34$ fm. For the obtained value of $< b >$, we have generated a total sample of 6200 events. From the analysis of generated events pions with dip angles greater than 60^0 have been excluded, because in the experiment the registration efficiency of such vertical tracks is low.

4 Kinematical characteristics of pions

We studied the kinematical characteristics of π^- mesons, produced in Mg-Mg collisions at a momentum of 4.3 GeV/c per nucleon, such as the average multiplicity, momentum, transverse momentum, emission angle, rapidity and corresponding distributions. In Table 1 the values of the $\langle n_- \rangle$, $\langle P \rangle$, $\langle P_T \rangle$, $\langle \Theta \rangle$, $\langle Y \rangle$ for the experimental data and events generated by the QGSM code for not fixed $\tilde{b}$ and $b = 1.34$ fm are listed. One can see, that the experimental and model values coincide within the errors. In Fig. 2-6 the corresponding experimental and generated distributions of n_-, P, Θ , P_T and Y are presented.

The comparison of these distributions allows to conclude, that the QGSM satisfactorily describes the spectra. The results obtained by the model in the two regimes are

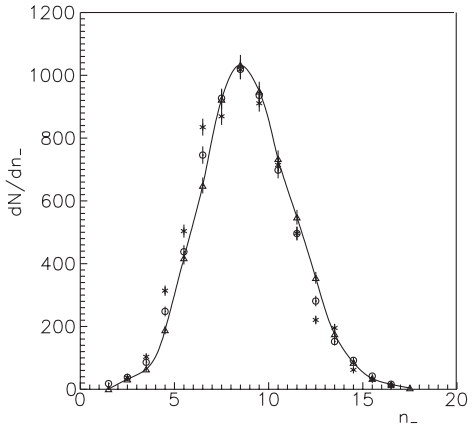

Fig. 2. The multiplicity distribution of π^- mesons. ∘ – the experimental data, curve △ – QGSM generated data for b=1.34 fm, ∗ – QGSM generated data for $\tilde{b}$

Table 2. The $\langle Y \rangle$ and dispersion D_Y for various intervals of P_T

		P_T<0.2	0.2≤P_T<0.3	0.3≤P_T<0.5	P_T≥0.5
experiment	$\langle Y \rangle$	1.23±0.01	1.22±0.02	1.22±0.02	1.20±0.02
	D_Y	1.16±0.02	0.95±0.01	0.85±0.02	0.70±0.01
QGSM					
b=1.34 fm	$\langle Y \rangle$	1.20±0.02	1.21±0.02	1.19±0.02	1.18±0.02
	D_Y	1.24±0.01	0.97±0.01	0.80±0.01	0.70±0.02

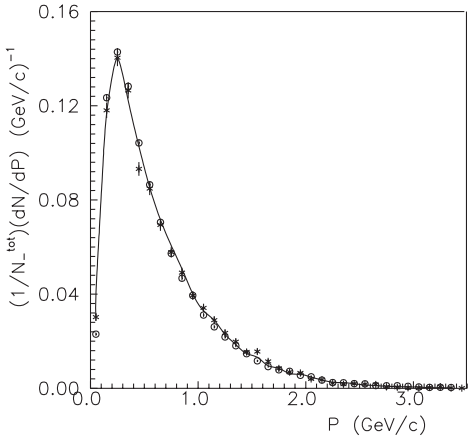

Fig. 3. The momentum distribution of π^- mesons. ∘ – the experimental data, curve – QGSM generated data for b=1.34 fm, ∗ – QGSM generated data for $\tilde{b}$

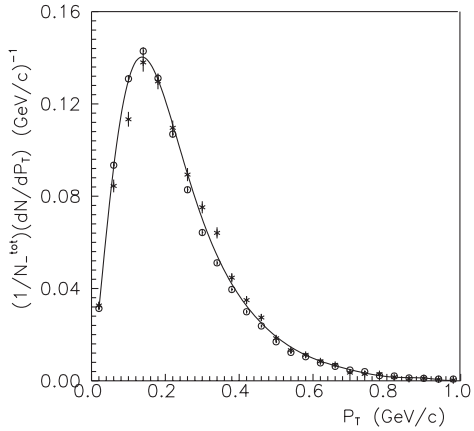

Fig. 5. The transverse momentum distribution of π^- mesons. ∘ – the experimental data, curve – QGSM generated data for b=1.34 fm, ∗ – QGSM generated data for $\tilde{b}$

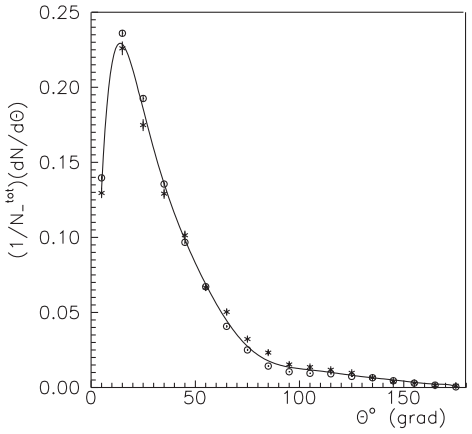

Fig. 4. The emmision angle distribution of π^- mesons. ∘ – the experimental data, curve – QGSM generated data for b=1.34 fm, ∗ – QGSM generated data for $\tilde{b}$

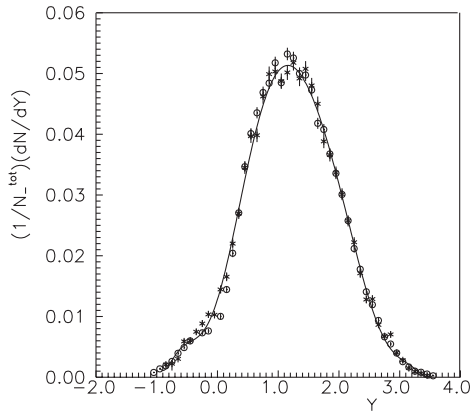

Fig. 6. The rapidity distribution of π^- mesons. ∘ – the experimental data, curve – QGSM generated data for b=1.34 fm, ∗ – QGSM generated data for $\tilde{b}$

consistent and it seems that in our experiment the value of $b = 1.34$ fm for Mg-Mg is most probable.

We used two Lorentz-invariant variables to describe the main features of the π^- mesons, produced in nucleus-nucleus collisions: the rapidity Y and the transverse momentum P_T. For this purpose we investigated rapidity distributions in various regions of P_T: $P_T \leq 0.2$, $0.2 \leq P_T < 0.3$, $0.3 \leq P_T < 0.5$, $P_T \geq 0.5$. The distributions (Fig.7) have the characteristic Gaussian form. The form of the Y distributions changes with increasing transverse momentum of π^- mesons: the fraction of pions increases in the central region and decreases in the fragmentation regime of the colliding nuclei. The Y distributions become narrower. The dispersion is changing from $D_Y = 1.16$ for $P_T \leq 0.2$ to $D_Y = 0.70$ for $P_T \geq 0.5$. The analysis of the Y distributions shows that the central regions of these distributions are enriched with pions of large transverse momentum (as compared to the fragmentation regions of the colliding nuclei): $\langle P_T \rangle = 0.184 \pm 0.004$ GeV/c for $Y < 0.2$, $\langle P_T \rangle = 0.247 \pm 0.002$ GeV/c for $0.7 \leq Y \leq 1.6$,

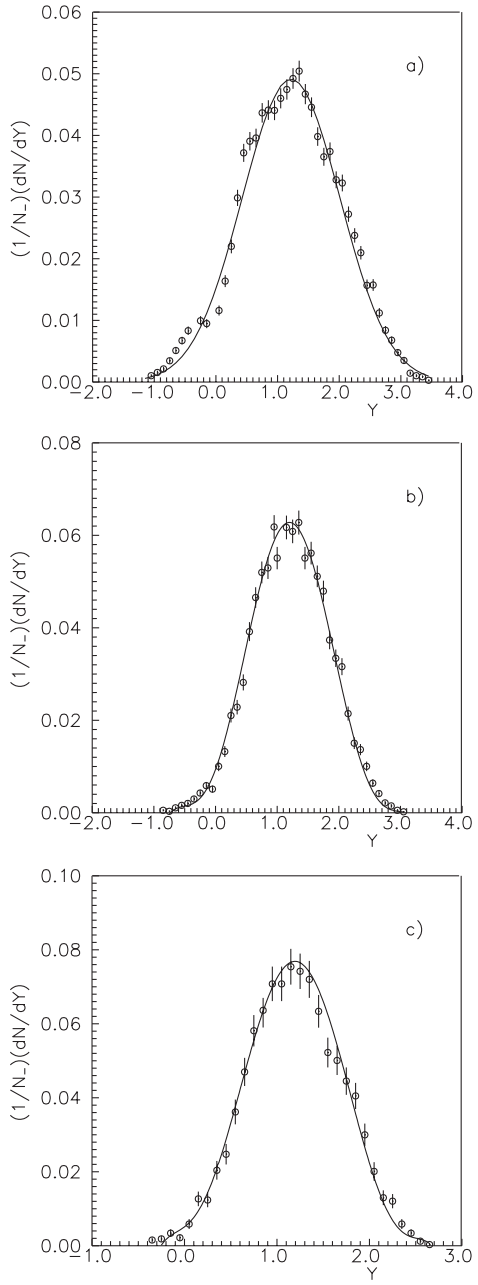

Fig. 7. The rapidity distribution of π^- mesons in various intervals of P_T. **a** $P_T < 0.2$; ∘ – the experimental data, curve – QGSM generated data for $b = 1.34$ fm. **b** $0.2 \leq P_T < 0.3$; ∘ – the experimental data, curve – QGSM generated data for $b = 1.34$ fm. **c** $P_T > 0.5$; ∘ – the experimental data, curve – QGSM generated data for $b = 1.34$ fm

$\langle P_T \rangle = 0.189 \pm 0.003$ GeV/c for $Y > 2$. The QGSM reproduces the Y distributions in the various regions of P_T well enough (Fig.7). The corresponding mean values of Y for experimental and model data are listed in Table 2.

Practically all theoretical models are based on the dependence of the average kinematical characteristics on the impact parameter b. As b is experimentally unmeasurable, the estimation of b may be obtained on the basis of the number of nucleons ν_p of the projectile participating in the interaction, which in turn is correlated with the multiplicity n_- of observed π^- mesons. Therefore the study of dependence of a given variable (P_T, etc) on b can be qualitatively replaced by the study of the dependence of the same variable on n_-.

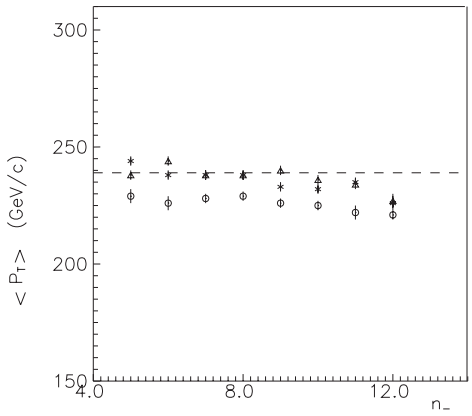

Fig. 8. The dependence of the average transverse momentum $< P_T >$ on the n_- variable. ∘ – the experimental data, △ – QGSM generated data for b=1.34 fm, ∗ – QGSM generated data for $\tilde{b}$. *Dashed line* shows the $< P_T >$ value for N-N collisions at 4.3 GeV/c

In Fig.8 the dependence of $< P_T >$ on n_- is presented. The dashed line corresponds to data, derived from the experiments on N-N collisions [10] at our energy (the values are averaged over all n_- values). One can see, that $< P_T >$ slightly decreases with multiplicity. In the model of independent collisions [11], nucleus-nucleus interactions are considered as a superposition of independent nucleon-nucleon collisions. In this case, the coincidence with the N-N collisions is expected. Figure 8 shows, that the QGSM reproduces these dependences well. The reason for some quantitative disagreement in $< P_T >$ may be attributed to nuclear effects, which are essential in Mg-Mg collisions.

5 The temperature of π^- mesons

An excited system of hadrons is characterized by its temperature. The π^- mesons temperature was estimated by means of: 1. spectra of inclusive kinetic energy E_K and 2. spectra of transverse momentum P_T.

Non-invariant inclusive spectra $d^3\sigma/d\boldsymbol{P} = (E^*P^*)^{-1} \cdot dN/dE_K^*$ (P^* is the momentum, E^*- the total energy and E_K^* the kinetic energy of the particle in the c.m.s.) have been analyzed. The experimental spectrum was fitted by a simple exponential law:

$$F(E_K^*) = (E^*P^*)^{-1} dN/dE_K^* = A_1 \cdot \exp(-E_K^*/T_1) + A_2 \cdot \exp(-E_K^*/T_2) \quad (3)$$

T is related to the average kinetic energy of a given type of particles and thus characterizes the nuclear matter temperature at the expansion stage when such particles are emitted. Therefore, the parameter T is usually called an average or inclusive temperature. The temperature may

Table 3. The temperatures of π^- mesons - result of approximation by (4) and (5)

A_P - A_T	Selection criteria	T_1 (MeV) T_2 (MeV) using (1)	T_1 (MeV) T_2 (MeV) using(2)
experiment	0.5≤Y≤2.1	55±1 113±2	61±1 110±3
QGSM b=1.34 fm	0.5≤Y≤2.1	52±8 103±1	66±7 95±5

also be deduced from transverse momentum distributions. This method was suggested by Hagedorn in the framework of the thermodynamic model [12,13]. This model assumes that in the collision process the hot sources (one or several) are formed and move together along the collision axis. Their longitudinal velocity and temperature obey energy-momentum conservation laws. Some authors [12-14] state that transverse momentum distributions are preferable because of their Lorentz-invariance in respect to longitudinal boosts. Transverse momentum distributions were described by [12-15]:

$$dN/dP_T \approx \text{const}\, P_T \cdot E_T \cdot (\exp(-E_T/T_1) + (\exp(-E_T/T_2)) \quad (4)$$

$$E_T = (P_T^2 + m^2)^{1/2}$$

The pion spectra can be well fitted by a sum of two exponentials (two temperatures T_1 and T_2). Experimental and generated spectra of the non-invariant kinetic energy E_{kin} and P_T have been approximated using formulas (3) and (4) in the rapidity interval $0.5 \leq Y \leq 2.1$, which corresponds to the pionization region. The fitted parameters are presented in the Table 3.

We can see from the table, that within errors parametrizations (3) and (4) give consistent results for T_1 and T_2. Calculated temperatures are consistent within both approaches, but the model underestimates the high temperature component by about $(10-15)\%$.

At our energy, the Hagedorn model [13] predicts only one temperature $T_{\pi^-} = (115-120)$ MeV, which agrees with our value of T_2. Several possible mechanisms have been proposed to explain two temperatures [7,16,17,18]. In [16] the presence of two temperatures for pions is explained by two mechanisms of pion production: direct (T_2) and via Δ resonance decay (T_1). In [17] the necessity of two temperatures is found to be caused by the different contributions of the Δ resonance produced during the early and the late stages of the nucleus-nucleus collisions, and due to the energy dependence of the pion and Δ absorption cross sections. In paper [18] this effect was quantitatively explained by taking into account the finiteness of the number of particles in the statistical ensemble and the resonance absorption mechanisms.

6 Transverse momentum analysis technique

The extraction of properties of the hot and dense hadronic matter from pion observables critically depends on our understanding of the pion-production dynamics. Hydrodynamical calculations predicted the formation of compression waves in nuclear matter in high energy heavy ion collisions [19]. Using the transverse momentum analysis technique developed by Danielewicz and Odyniec [20], nuclear collective flow has already been observed for protons, light nuclei and Λ–hyperons emitted in nucleus-nucleus collisions at energies 0.4÷1.8 GeV/nucleon at the BEVALAC, GSI-SIS [21-24], and at 11÷14 GeV/nucleon at AGS [25,26]. Due to the small mass of pions compared to that of baryons, it has been pointed out that the pions might serve as a good probe of any hydrodynamical flow [27]. Moreover, as pions are mainly coming from the decay of Δ resonances in relativistic nucleus-nucleus interactions, the remnant of the collective flow carried by Δ resonances might be seen in the distributions of the final state pions. In search for collective flow signatures among final-state pions the transverse momentum technique has also been applied to pions from relativistic nuclear reactions [21,23]. Looking for flow effects in pion emission, they have measured the correlation between the reaction plane, deduced from a transverse-momentum analysis performed on light baryons (protons), and the momenta of charged pions emitted in collisions.

P. Danielewicz and G. Odyniec have proposed an exclusive way to analyse the momentum contained in direct sidewards emission and presented the data in terms of the mean transverse momentum per nucleon in the reaction plane $< P_x(Y) >$ as a function of the rapidity. The reaction plane is determined by the vector $\overrightarrow{Q_j}=\sum_{i\neq j}^{n}\omega_i\ \overrightarrow{P_{\perp i}}$ and the incident beam direction. Here $P_{\perp i}$ is the transverse momentum of particle i, and n is the number of particles in the event. Pions are not included. The weight ω_i is taken as 1 for $y_i > y_{cm}$ and -1 for $y_i < y_{cm}$, where y_{cm} is the c.m.s. rapidity and y_i is the rapidity of particle i. The transverse momentum of each particle in the estimated reaction plane is calculated as $P'_{xj} = \{\overrightarrow{Q_j} \cdot \overrightarrow{P_{\perp j}}/|\overrightarrow{Q_j}|\}$.

The average transverse momentum $< P_x'(Y) >$ is obtained by averaging over all events in the corresponding intervals of rapidity.

For Mg-Mg collisions we have inclusive data - only π^- mesons are measured. As the π^- mesons are emitted mainly from decays of Δ isobars (at least $\sim 80\%$) [28], we decided to investigate whether a single π^- meson of the event knows something about its origin and the question whether they are collectively correlated. For this purpose we applied the technique of P. Danielewicz and G. Odyniec to our data. As we have inclusive data, we constructed the

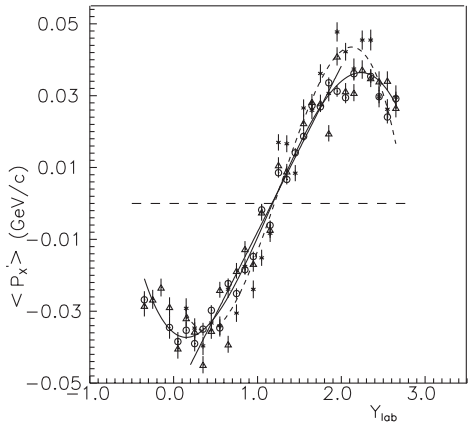

Fig. 9. The dependence of $< P'_x(Y) >$ on Y_{Lab}. $\circ$ – the experimental data, $\triangle$ – the QGSM generated data for fixed $b = 1.34$ fm, $*$ – the QGSM generated data for $\tilde{b}$. The solid line is the result of the the linear approximation of experimental data in the interval of $Y - 0.2 \div 2.0$. The *curves* for visual presentation of the QGSM events (*solid* – for fixed b, *dashed* – for $\tilde{b}$) – result of approximation by 4-th order polynomial function

$\overrightarrow{Q}$ vector from the $\overrightarrow{P_{\perp i}}$ of only π^- mesons event by event for the events with multiplicity $n_- > 7$.

It is known [20], that the estimated reaction plane differs from the true one, due to the finite number of particles in each event. The component P_x in the true reaction plane is systematically larger then the component P'_x in the estimated plane, hence $< P_x >=< P'_x > / < \cos\varphi >$ where φ is the angle between the estimated and true planes. The correction factor $K = 1/ < \cos\varphi >$ is subject to a large uncertainty, especially for low multiplicity. According to [20], for the definition of $< \cos\varphi >$ we divided each event randomly into two equal sub-events, constructed vectors $\overrightarrow{Q_1}$ and $\overrightarrow{Q_2}$ and estimated azimuthal angle $\varphi_{1,2}$ between these two vectors. $< \cos\varphi >=< \cos(\varphi_{1,2}/2) >$. We defined the correction factor K, averaged over all the multiplicities. A value of $K = 1.51 \pm 0.05$ has been obtained.

Figure 9 shows the dependence of the estimated $< P'_x(Y) >$ on Y for pions. The data exhibit S- shape behaviour similar to the form of the $< P_x >$ spectra for protons [21,22,24] and pions [21,23] obtained at lower energies and identified as nucleon and pion collective flow. The slope at midrapidity has been extracted from a linear fit to the data for Y between $0.2 \div 2$. The straight line in Fig. 9 shows the result of this fit. The value of F is – $F = 48 \pm 5$ (MeV/c). F is normally lower than the true value because $P'_x < P_x$, thus the obtained value of the parameter F can be considered as a lower limit. In the model calculations the reaction plane is known a priori and is refered as the true reaction plane. For simulated events the component in the true reaction plane P_x had been calculated. The dependences of $< P_x(Y) >$ on Y (for both $\tilde{b}$ and b) are shown in Fig. 9. The experimental and QGSM results coincide within errors. For the visual presentation, we approximated these dependences by polynoms (the curves in Fig. 9). From the comparison of the dependences of $< P_x(Y) >$ on Y obtained by the model in two regimes - for $\tilde{b}$ and b, one can conclude, that the results are consistent. The values of F, obtained from the QGSM are: $F = 53 \pm 3$ (MeV/c) — for not fixed $\tilde{b}$; $F = 51 \pm 4$ (MeV/c) — for $b = 1.34$. One can see, that the QGSM underestimates this parameter, as the value of F from the experimental data is a lower limit, because it is not multiplied with the uncertainty factor K.

The origin of the particular shape of the P_x spectra for pions had been studied in [28-30]. The investigation revealed, that the effect of baryon collective flow on the pion transverse momentum distribution is negligible and the origin of the in-plane transverse momentum of pions is not the remnant of the Δ flow [29], but the pion scattering process (multiple πN scattering) [28] and the pion absorption [29,30]. The $< P_x >$ distribution of pions is not a collective effect in the sense of the nucleonic bounce-off: the observable is the same, but the cause is different.

In the framework of the Isospin Quantum Molecular Dynamics (IQMD) model [28] and the hadronic BUU transport model [30] it had been obtained, that in central Au-Au collisions ($b \leq 3\ fm$) at $E = 1 - 2$ GeV/n and La-La collisions at $E = 0.8$ GeV/n the pion average transverse momentum $< P_x >$ have the same sign as that of nucleons in both forward and backward rapidities. The correlation of nucleon and pion flow had been observed experimentally by the DIOGENE group for central Ne-NaF, Ne-Nb and Ne-Pb collisions ($b \leq 3\ fm$) at $E = 0.8$ GeV/n [23]. These results are in agreement with our findings. With increase of the impact parameter b, the $< P_x >$ of pions changes its sign [28,30]. Therefore as reaction goes from central to semicentral and peripheral ($b \geq 4\ fm$) the $< P_x >$ distribution of pions undergoes a transition from being correlated to anticorrelated with that of nucleons. The anticorrelation of nucleons and pions in [28] was explained as due to multiple π N scattering. However in [30] it had been shown, that the anticorrelation is a manifestion of the nuclear shadowing effect of the target- and projectile-spectator through both pion rescattering and reabsorptions.

7 Conclusions

A study of pion production in central Mg-Mg collisions was carried out.

1. The average kinematical characteristics of pions such as multiplicity, momentum, transverse momentum, emission angle, rapidity and corresponding distributions have been obtained. The QGSM satisfactorily describes the experimental results.

2. It has been shown, that $< P_T >$ slightly decreases with multiplicity. This average kinematical characteristics are similar to the characteristics of N-N collisions at the same energy. The reason of some quantitative disagreement in $< P_T >$ may be attributed to the nuclear effects, which are essential in Mg-Mg collisions. The QGSM reproduces the dependence of $< P_T >$ on n_-.

3. The temperature of π^- mesons has been determined from E_K and P_T spectra in the rapidity interval $0.5 \leq Y \leq 2.1$. The sum of two exponentials is necessary to reproduce the data. The temperatures have been obtained from spectra generated by QGSM. It underestimates T_2 about (10-15) %.

4. The data have been analyzed event by event using transverse momentum technique. The results are presented in terms of the mean transverse momentum $< P'_x(Y) >$ as a function of the Y. The observed dependence of the $< P'_x(Y) >$ on Y shows the S-shape behaviour. The slope at midrapidity F had been extracted. The QGSM reproduces the $< P_x >$ distribution, but underestimates the parameter F.

We would like to thank professor N.Amaglobeli for his continuous support. We are indebted to M. Anikina , A. Golokhvastov, S. Khorozov, J. Lukstins, L. Okhrimenko for helping in obtaining the data and many valuable discussions. We are very grateful to N.Amelin for providing us with the QGSM code program COLLI, also to Z. Menteshashvili for his continuous support during the preparation of the article and reading the manuscript.

The research described in this publication was made possible in part by Grant MXP000 from the International Science Foundation and Joint Grant MXP200 from the International Science Foundation and Government of Republic of Georgia.

References

1. M.X. Anikina et al: Phys. Rev. C**33** (1996) 895
2. L.V. Chkhaidze et al: Z. Phys. C**54** (1992) 179
3. L.V. Chkhaidze et al: J. Phys. G**22** (1996) 641
4. N. Amelin et al: Yad. Fiz. **52** (1990) 272
5. N. Amelin et al: Phys. Rev. C**44** (1991) 1541
6. S. Nagamiya and M. Gyulassy: Adv. in. Nucl. Phys. **13** (1984) 201 and references therein
7. B.A. Li and W. Bauer: Phys. Rev. C**44** (1991) 450
8. M.D. Zubkov: Yad. Fiz. (Soviet Journal of Nuclear Physics) **55** (1989) 455
9. V.V. Anisovich et al: Nucl. Phys. B**133** (1978) 477
10. K. Beshliu et al: Yad. Fiz. **43** (1986) 808
11. S.A. Khorozov: JINR Dubna Report 2-80142 (1980)
12. R. Hagedorn: CERN Geneva Preprint TH-**3684** (1984) 59
13. R. Hagedorn: Phys. Lett. B**97** (1980) 136
14. V. Gudima et al: Phys. Elem. Part. At.Nucl. **17** (1986) 1093
15. R. Stock: Phys. Rep. **135** (1986) 261
16. S. Nagamiya: Phys. Rev. Lett. **49** (1982) 1383
17. D. Hahn and N. Glendenning: Phys. Rev. C**37** (1988) 1053
18. M.D. Zubkov: Yad. Fiz. **49** (1989) 1751
19. H. Stocker and W. Greiner: Phys. Rep. **137** (1986) 277 and references therein
20. P. Danielewicz and G. Odyniec: Phys. Lett. B**157** (1985) 146
21. P. Danielewicz et al: Phys. Rev. C**38** (1988) 120
22. O. Beavis et al: Phys. Rev. C**45** (1992) 299
23. J. Gosset et al: Saclay Rapport DPh-N/Saclay; **2469B** (1987) 5
    J. Gosset et al: Phys. Rev. Lett. **62** (1989) 1251
24. S. Albergo et al: Nucl. Phys. **A590** (1995) 549c
25. T. Abbott et al: Phys. Rev. Lett. **70** (1993) 1393
26. J. Barrette et al: Phys. Rev. Lett. **73** (1994) 2532
27. P. Siemens and J. Rasmussen: Phys. Rev. Lett. **42** (1979) 880
28. S. Bass et al: Phys. Rev. C**51** (1995) 3343
29. B.A. Li, W. Bauer and G. Bertsch: Phys. Rev. C**44** (1991) 2095
30. B.A. Li: Nucl. Phys. A**570** (1994) 797